MAGNETOHYDRODYNAMICS Vol. 00 (1964), No. 00, pp. 1–??

Effects of Size and Stretch of a Moving Ferrofluid Drop to Induced Electromotive Force

Ching-Yao Chen[1,†], *Sheng-Yan Wang*[1], *Chih-Yung Wen*[2] *and Cheng-Shiung Jan*[1]

Department of Mechanical Engineering, National Chiao Tung University, Hsinchu, Taiwan, Republic of China

Department of Mechanical Engineering, Hong Kong Polytechnic University, Hong Kong, China

[†] *Email:chingyao@mail.nctu.edu.tw*

Application for obtaining useful global features, e.g., size and stretch, of a moving ferrofluid drop by analyzing the characteristics of induced electromotive force (EMF) signal is demonstrated. These features are highly relevant to two maximum magnitudes in the EMF signal, e.g., positive (V_1) and negative (V_2) peak respectively induced when the drop enters and leaves the region covered by the induction coil. Favorable induction conditions of these two maximum magnitudes are oppositely. In general, V_1 increases with size of the ferrofluid drop because of stronger magnetization. On the contrary, V_2 is more prominent for a smaller drop, whose stretch is less significant. As a result, the ratio of $|V_1/V_2|$ monotonically increases with the size of ferrofluid drop. This finding suggests that the induced EMF signal can be used as a useful tool for quantifying the flow conditions, such as the size and stretch of moving ferrofluids.

1. Introduction and experimental setup Ferrofluid is a remarkable class of smart materials, whose particles are nanometer-sized and coated by surfactants. Conventional applications of ferrofluid in the industry had been well-established, e.g., multistage rotary seals, inertial dampers and loudspeakers [1, 2]. New applications are implemented in the domains of micro-technology [3], and materials as well as biomedicine [4].

On the other hand, it is well known by the Faraday law that electromotive force (denoted as EMF thereafter) is induced in responding to an unsteady motion of magnetized materials. The induced EMF can be obtained by the Faraday Law as

$$EMF = -N_c \frac{d\phi}{dt}, \tag{1}$$

$$\phi = \int (\mathbf{B} \cdot \mathbf{n}) dA, \tag{2}$$

where N_c, ϕ, and t stand for the number of identical turns of induction coil, magnetic flux, and time, respectively. $\mathbf{n}$ and A represent a unit normal vector and the area. The magnetic induction field $\mathbf{B}$ can be further expressed by

$$\mathbf{B} = \mu_0(\mathbf{H} + \mathbf{M}), \tag{3}$$

in which μ_0, $\mathbf{H}$ and $\mathbf{M}$ are the permeability of vacuum, the magnetic field strength, and the magnetization of ferrofluids, respectively. It is apparent that both the temporal variations of the magnetic induced field and the effective area, in which perpendicular to the magnetic flux, are able to generate EMF. Devices for measuring the concentration and dispersion quality of magnetic particles by the induced EMF had been suggested since several decades ago [5]. Similar studies but using

ferrofluids had been conducted both experimentally and theoretically [6]. The reverse situation of liquid motion driven by the thermoelectric current and magnetic field interaction had also been studied [7]. In recent years, new techniques have been proposed to measure the void fractions and velocities of bubbles in the gas-liquid (or gas-ferrofluids) flow system by their electromagnetic induction [8, 9, 10]. In addition, understandings of the characteristics of electromagnetic induction are also crucial if an electricity conversion device from the moving magnetic fluids is desired [11, 12]. To gain more fundamental understandings of the electromagnetic induction of moving ferrofluids, experiments for un-deformable ferrofluids contained in a small bottle with constant speed has been performed [13]. Magnitudes of induced EMF for various volumes and shapes (i.e., aspect ratio of containers) of ferrofluid subjected to different external field strengths are analyzed. The results could be potentially applied to characterize the motion of well controlled ferrofluids.

In this work, we experiment more practical situations, in which the EMF is induced by a deformable magnetized ferrofluid drop driven by the attraction of permanent magnets. We focus on the influences of relevant physical conditions, such as external field strength and size of ferrofluid drop, to the characteristics of correspondent EMF signal. To elucidate the corresponding behaviors of the ferrofluid drop, parallel experiments without induced coil are carried out as well, so that the motion of ferrofluid drop can be clearly observed. The results are expected to provide insight information to flow diagnosis by the EMF signal.

The experimental setup consists of a glass tube and induction coil, as depicted in Fig. 1. The glass tube, whose diameter is 12 mm, is filled with mixture of glycerol and water to match the density of experimented ferrofluids. A ferrofluid drop, which is commercial light mineral oil based ferrofluids (EMG905) produced by the Ferrotec Corp, with volume of $\forall_f$ is then placed in the tube above the coil. The ferrofluid drop is pulled downwardly by permanent magnets on the bottom of the tube. Number of magnets used in different experiments is denoted by N. The tube is placed through the inner hole of an induction coil, whose outer and inner diameter is 78 mm and 15 mm, respectively. The height of the induction coil is L_c =51 mm, and contained 2160 turns of 0.6 mm-diameter wire. A gaussmeter probe is placed on the top of coil to record the local magnetic flux density. The measurements of magnetic flux density and induced EMF are recorded by a data logger and transmitted directly to a personal computer (PC) for further analysis. By the present experimental setup, images of the moving drop are blocked by the coil, so that parallel experiments without coil are also conducted to record the images by a CCD camera.

2. Results and Discussion

2.1. Representative cases The results of a representative series of various volumes subjected to different magnetic field strengths (or numbers of magnets) are first presented to elucidate the distinct features of induced EMF signals. Shown in Fig. 2 are the images of a moving ferrofluid drop of $\forall_f$=0.40 ml attracted by 6 permanent magnets ($N = 6$) for two experiments with/without the induction coil. Also shown in Fig. 2 is the external magnetic field distribution of magnets, referred to as the background field hereafter in. The parallel experiment without the induction coil is used for better observations of motion and deformation of the ferrofluid drop. On the other hand, induced EMF is recorded by the experiment with the coil, and shown in Fig. 3. Also shown in Fig. 3 is the magnetic induc-

tion field directly measured by the gaussmeter placed on the top of the induction coil. Subjected to the attraction of magnets, the initially nearly circular drop is stretched and driven to move downward. At a reference time t_A, when the drop locates sufficiently distant from the top of the coil, the magnetic induction field remains almost the same as the background field. As a result, no significant magnetization and EMF is induced. Because of greater gradient of the background field as the drop moving further downward, stretch of the drop is more prominent when it partially enters the region covered by the coil at t_B. In addition, the stronger local field strength enhances the magnetization, so that measured strength of the magnetic induction field starts to deviate from the background field, and EMF is induced consequently. The trend keeps evolving, e.g., more prominent stretch of the drop, stronger magnetization and induced EMF, till the EMF reaches maximum at t_C, denoted as V_1. Afterward, the growth rate of the magnetization decreases, so that EMF decays to zero at t_D when the magnetization is in its maximum. The growth rate of magnetization turns negatively to induce negative EMF and reaches its maximum magnitude at t_E, denoted as V_2. It is noticed that the drop remains highly stretched at t_D and t_E. Similar decay of EMF occurs when the negative growth rate of magnetization becomes milder. At t_F, almost all the ferrofluids reach bottom of the tube, and measured strength of the magnetic induction field returns to nearly background field without significant induced EMF. We like to point out that, even the general pattern of the EMF signal with maximum positive and negative magnitudes is consistent with the cases presented in Ref. [13], in which ferrofluids move in a constant speed without deformation, the present signal does not appear symmetrically, e.g., $|V_1| > |V_2|$. The asymmetry of EMF signal clearly indicates strong influences of unsteady motion and significant stretch of the moving drop to the EMF signal. To further realize the induction signal, a smaller drop subjected to fewer magnets is experimented, e.g., $\forall_f$=0.20 ml and N=3 shown in Fig. 4, in which the total magnetic effects are weaker, e.g., magnetization strength and magnetic attraction. It is very interesting to notice that a distinct feature of the EMF signal is resulted. Even the asymmetry is still preserved, the maximum magnitude of EMF appears at the negative peak, i.e., $|V_1| < |V_2|$. To verify the trend, a case with even weaker magnetic effects are tested, e.g., $\forall_f$=0.05 ml and N=1 shown in Fig. 5. Consistent result is obtained to conclude that, the ratio between the peak magnitudes of induced EMF, i.e., $|V_1|/|V_2|$, depends strongly on the magnetic effects. These interesting observations suggest potential applications of the EMF signal to characterize the drop motion.

2.2. Characterization of EMF Signal To better realize the features of the induced EMF signals, underlined mechanisms for electromagnetic induction are worthy for detailed discussion. According to the Faraday law, the EMF is induced by the unsteady magnetic effects, so that stronger magnetization is generally favorable. Since the magnetized strength is affected by the local magnetic field strength and volume of the magnetized fluids, magnetization is always stronger for a bigger drop approaching closer the magnets. As shown in Figs. 2 and 3, the measured magnetic induction field starts to rise when the drop is about to enter the induction coil at t_B to induce distinguishable positive EMF. The induced EMF keeps increasing to its maximum V_1 at t_C, because of more magnetized ferrofluids reaching within and passing through the induction coil. Afterward, the induced EMF shows decrease when major portion of magnetized fluids leave out the region of coil, so that opposite sign of EMF is induced as the negative peak V_2 occurring at t_E. The induced EMF eventually vanishes when all the ferrofluids have

completely passed through the coil. The overall scenario is generally similar with the cases presented in Ref. [13]. Nevertheless, somehow unexpected is a smaller magnitude of the negative peak, i.e., $|V_1| > |V_2|$, since the local background field is stronger at t_E due to shorter distance away from the magnets. The reason for this unexpected result is attributed to drop deformation, or longer stretched length L_d, of the drop. As demonstrated in Fig. 2, the magnetic attraction, which is relevant to the field gradient, increases as the drop moves further downward. The drop is highly elongated after t_c. This stretched drop results in milder unsteady effect, or rate, of local magnetization within the region covered by the coil, so that the magnitude of induced EMF appears lower even the local magnetization is stronger. This explains the reason of greater magnitudes of positive induced EMF, i.e., $|V_1| > |V_2|$, for a larger drop with significant stretch. On the other hand, for smaller drops, e.g., cases shown in Figs. 3 and 4, the positive induced EMFs are lower at the time when drops enter and pass through the coil, because of weaker effective magnetizations associated with smaller volumes of ferrofluids. Nevertheless, the stretches of these drops are less prominent at the later stage when the drops leave the coil, so that the effective rates of magnetizations to the region covered by the coil is relatively higher. Consequently, higher induced EMF occurs at the later stage when the ferrofluids leave the coil, and reverse feature of induced EMF signals is resulted, i.e., $|V_1| < |V_2|$.

The results presented above suggest that the maximum magnitudes of positive and negative induced EMF are mainly dominated by volume and stretch of the drop, respectively. To further verify the arguments, series of experiments with a fixed background field strength, e.g., N=6, for different drop sizes are presented. It is noticed that, multiple experiments are carried out for each conditions, and the results are represented by their means. The correspondent maximum magnitudes of positive and negative EMF for various values of $\forall_f$= 0.05 $\sim$ 0.40 ml are shown in Fig. 6. The maximum positive induced EMFs show monotonically increase, which are in line with the expectation. As for the negative induced EMFs, the maximum magnitudes increases for cases of relatively small drops, e.g., $\forall_f \leq 0.10$ ml, followed by a decreasing trend for cases of larger drops, e.g., $\forall_f \geq 0.10$ ml. The inconsistency for smaller sizes of drops ($\forall_f \leq 0.10$ ml) can be explained by domination of magnetization. As mentioned in the previous paragraph, both the positive and negative inductions, without the influences of drop stretch, are expected to increase as volume of the drop is larger. For smaller drops, the drop stretch is less prominent, so that the influences to lower the negative induced EMF are less significant. On the other hand, the effects of increasing ferrofluid volume which enhances the induced EMF are relatively more significant. As a result, increasing EMFs are observed associated with larger volumes for the case with relatively smaller sizes of drops, e.g., $\forall_f \leq 0.10$ ml. Nevertheless, stretches of the ferrofluids at later stage, which tend to reduce the negative EMFs, are more prominent as the drops become bigger, e.g., the stretched length L_d for various drop sizes shown in Fig. 7. When the drop exceeds a certain critical size, the influences of stretches to weaken EMFs would eventually dominate, and lead to decrease of the negative EMFs as shown for cases of $\forall_f \geq 0.10$ ml. The competition between the stronger magnetization and prominent stretch of the ferrofluids to the negative EMFs explains the non-monotonic behavior shown in Fig. 6.

For the cases reported above, we conclude that features of the EMF signals, e.g., the maximum magnitudes of the positive and negative EMFs, are highly relevant to the drop conditions, such as the original sizes and the stretched behaviors during the motion. For many practical conditions whose observations of flow fields are difficult, it would be beneficial if the forth mentioned global flow conditions,

e.g., sizes of moving ferrofluids, can be obtained by analyzing the easy-accessed EMF signals. Shown in Fig. 8 are the ratios of the peak magnitudes of EMF signals ($|V_1/V_2|$) for various sizes of ferrofluid drops. An interesting monotonic increase of the ratio is obtained. This monotonic trend is the aftermath of the arguments discussed above. On the one hand, a larger drop is always associated with stronger magnetization to result in higher $|V_1|$ at early stage, in which the stretch is not prominent. On the other hand, the larger drop tends to result in prominent stretch at later stage to reduce $|V_2|$. Consequently, the value of $|V_1/V_2|$ would monotonically increase with the volume of ferrofluid drop.

3. Concluding remarks In this work, we experimentally study the characteristics of electromagnetic induction of a magnetized ferrofluid drop attracted by magnets to pass through an induction coil. To better observe motion of the drop, parallel experiments in identical conditions without the induction coil are also carried out. Because of acceleration and deformation when the drop approaches the magnets, signal of the induced electromotive force (EMF) appears asymmetrically. This asymmetry of EMF signal provides useful information for potential flow diagnosis. We focus on the maximum magnitudes of EMF signals, e.g., the positive (V_1) and negative (V_2) peak value respectively induced at the early and late stage. Magnitude of (V_1) is predominated by the magnetization strength, which increases with size of the ferrofluid drop. On the contrary, magnitude of (V_2) is weakened if stretch is prominent, which is favorable for a larger drop. As a result, the ratio of $|V_1/V_2|$ increases monotonically with size of the ferrofluid drop. This fact provides very useful information for quantifying the global flow conditions by analyzing the EMF signal, such as size and stretch of the moving ferrofluid drop.

4. Acknowledgments Supports by the Ministry of Science and technology of the Republic of China (Taiwan) under grant MOST 104-2221-E-009-142-MY3 is acknowledged.

REFERENCES

1. R.E. Rosensweig, Ferrohydrodynamics? Cambridge University Press, Cambridge, England (1985).
2. E. S. Blums, A. O. Cebers, M. M. Maiorov, Magnetic Fluids? Walter de Gruxter, New York (1997)
3. N. T. Nguyen, Micro-magnetofluidics: interactions between magnetism and fluid flow on the microscale. Microfluid Nanofluid 12:1-16 (2012).
4. C. Scherer and A. M. Figueiredo Neto, Ferrofluids: Properties and Applications? Brazilian Journal of Physics 35: 718-727 (2005).
5. T. M. Kwon, M. S. Jhon, and T. E. Karis, A device for measuring the concentration and dispersion quality of magnetic particle suspensions,?IEEE Transactions on Instrumentation and Measurement 41, 1, 10-16 (1992).
6. A. A. Kubasov, Electrmotive force generation due to ferrofluid motion,?Journal of Magnetism and Magnetic Materials 193, 15-19 (1997).
7. I. Kaldre, Y. Fautrelle, J. Etay, A. Bojarevics and L. Buligins, Investigation of liquid phase motion generated by the thermoelectric current and magnetic field interaction. Magnetohydrodynamics 46, 4, 371-380 (2010).
8. S. Shuchi, H. Yamaguchi and M. Takemura, Measurement of void fraction in magnetic fluid using electromagnetic induction,?J. Fluids Eng. 125, 479 (2003).

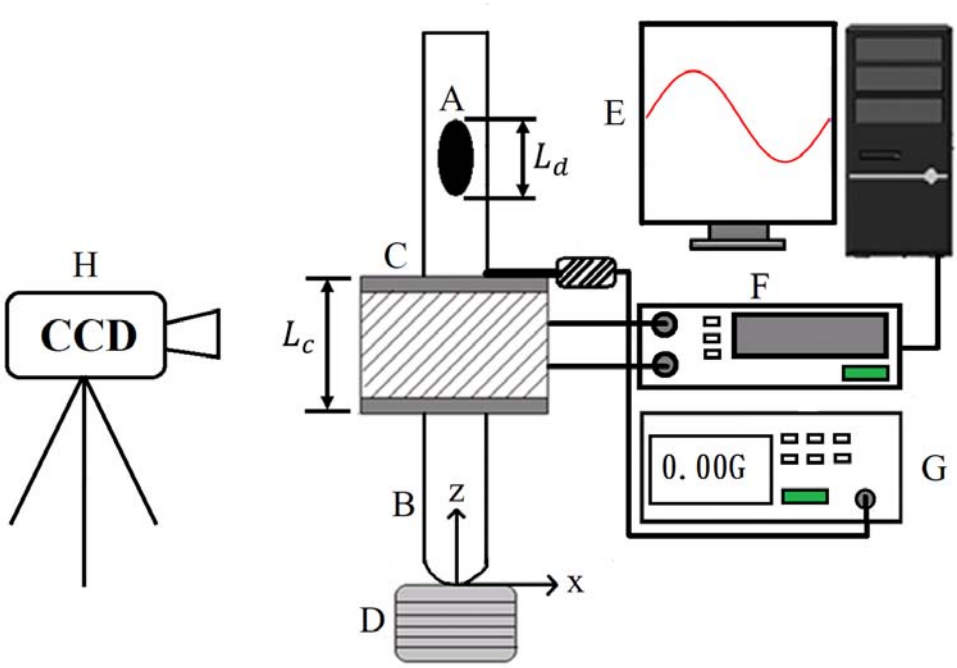

Figure 1: Principle sketch of experimental setup. A : ferrofluid drop ; B : glass tube ; C : induction coil ; D : magnets ; E : personal computer ; F : data capturer ; G : Gaussmeter ; H : CCD camera. L_d and L_c are longitudinal lengths of the stretched ferrofluid and induction coil, respectively. A ferrofluid drop, initially suspended in a surrounding fluid with identical density, is attracted by the magnets to move downward and pass through the induction coil.

9. T. Kuwahara, and H.Yamaguchi, Void fraction measurement of gas-liquid two-phase flow using magnetic fluid,?J. Thermophys. Heat Transf. 21, 173 (2007).
10. T. Kuwahara, F. De Vuyst, and H.Yamaguchi, Bubble velocity measurement using magnetic fluid and electromagnetic induction,?Phys. Fluids 21, 097101 (2009).
11. F. Gazeau, C. Baravian, J.-C. Bacri, R. Perzynski, and M. I. Shliomis, Energy conversion in ferrofluids: Magnetic nanoparticles as motors or generators, Phys. Rev. E 56, 614?18 (1997).
12. S. Carcangiu, A. Montisci and R. Pintus, Performance analysis of an inductive MHD generator. Magnetohydrodynamics 48, 1, 115-124 (2012).
13. C.-Y. Chen, S.-Y. Wang, C.-M. Wu, C.-H. Lin, and K.-A. Huang, Characteristics of Electromagnetic Induction by Moving Ferrofluids? Magnetohydrodynamics 48, No. 3, 567-580, 2012.

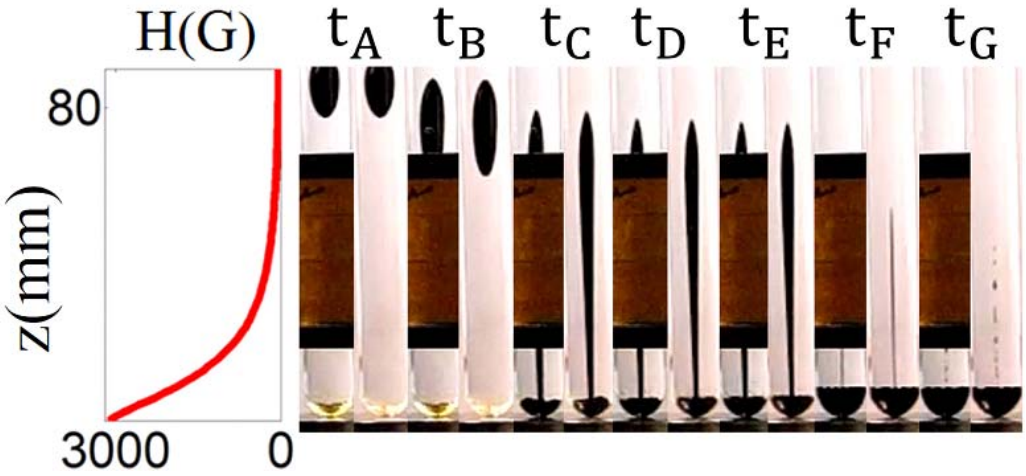

Figure 2: Images of ferrofluid drop with volume of $\forall_f$=0.40 ml attracted by 6 magnets ($N = 6$)at different times $t_A \sim t_G$. Shown in the left is the distribution of external magnetic field strength along the vertical distance, denoted by z, away from the magnets. Two experiments with identical conditions with and without the induction coil are respectively demonstrated in the left and right. The case with induction coil is used to measure the induced electromotive force (EMF), while detailed motion of the ferrofluid drop is observed by the experiment without the induction coil.

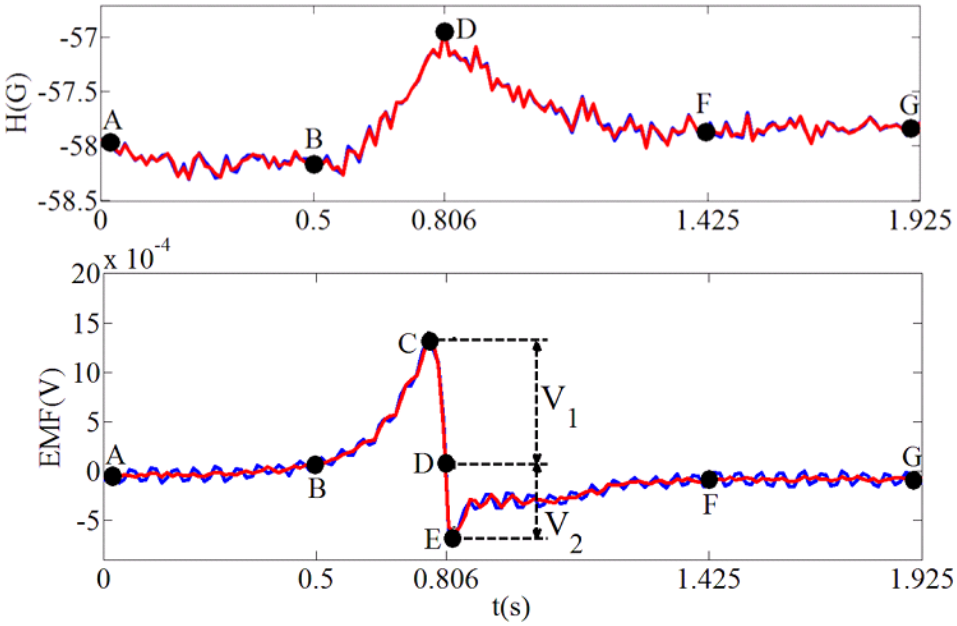

Figure 3: Evolutions of magnetic induction field strength (top) and induced EMF (bottom) for the experiment shown in Fig. 2, i.e., $N = 6$ and $\forall_f$=0.40 ml. Points $A \sim G$ correspond the times of $t_A \sim t_G$ shown in Fig. 2. The induction field strength is measured on the top of induction coil as mark G in Fig. 1. The original measured values are plotted by blue curves, and smoothed by FFT filter as shown by the red curves. V_1 and V_2, which respectively occur at t_C and t_E, represent the positive and negative peak EMF magnitudes, respectively.

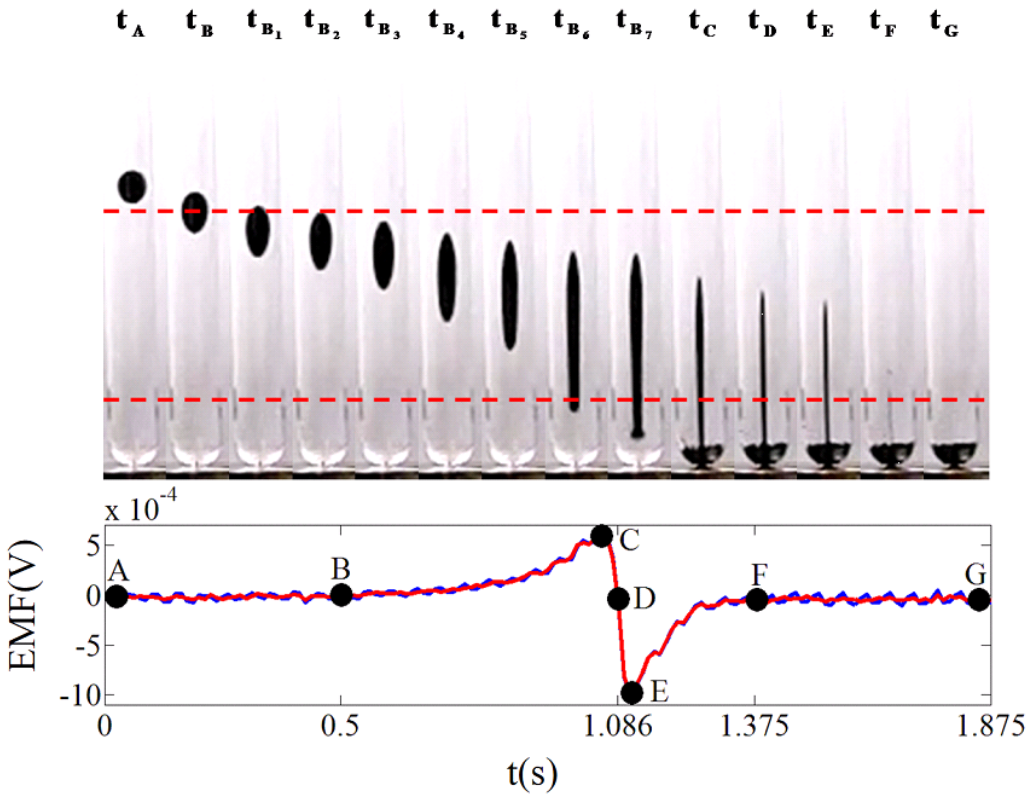

Figure 4: Images of the ferrofluid drop(top) and evolution of induced EMF (bottom) for the case of $N = 3$ and $\forall_f$=0.20 ml. The region of induction coil in the corresponding experiment for obtaining EMF is indicated by red dash lines.

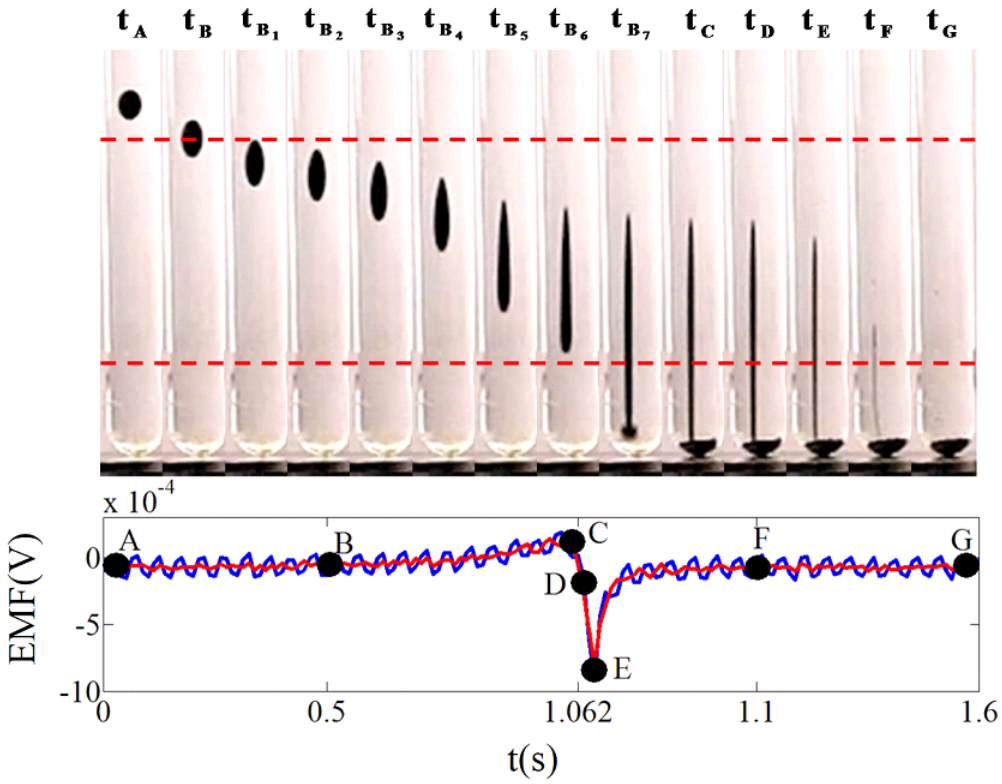

Figure 5: Images of the ferrofluid drop(top) and evolution of induced EMF (bottom) for the case of $N = 1$ and $\forall_f$=0.05 ml. The region of induction coil in the corresponding experiment for obtaining EMF is indicated by red dash lines.

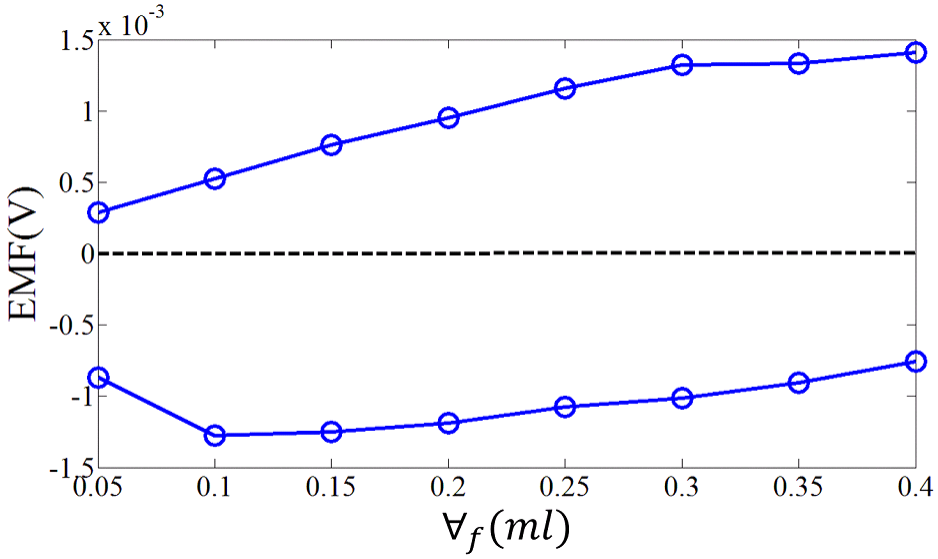

Figure 6: Positive and negative peak EMF values for various volumes of ferrofluid drop ($\forall_f$) driven by 6 magnets ($N = 6$).

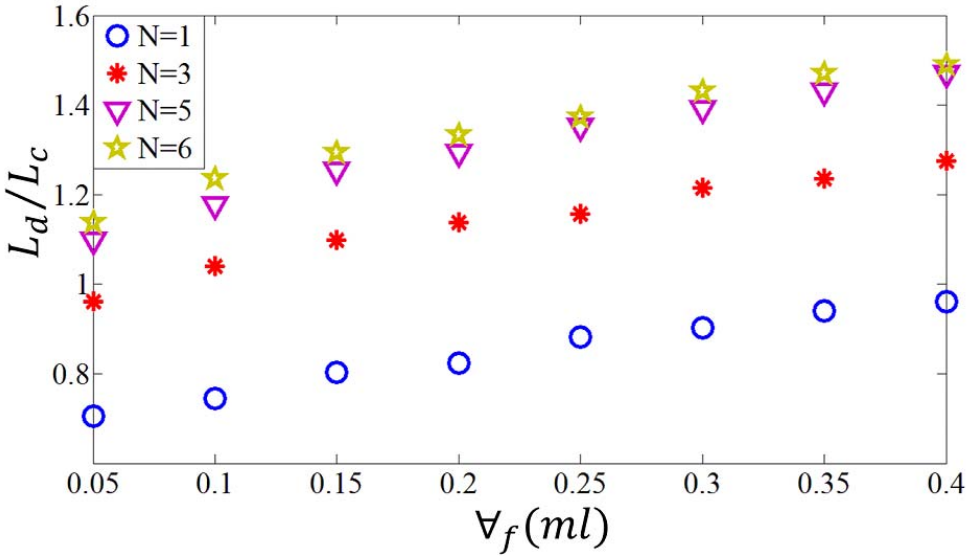

Figure 7: Normalized maximum stretched drop length, denoted as L_d/L_c measured at the time when ferrofluids reach bottom of the tube, for various conditions of drop volumes ($\forall_f$) and number of magnets (N).

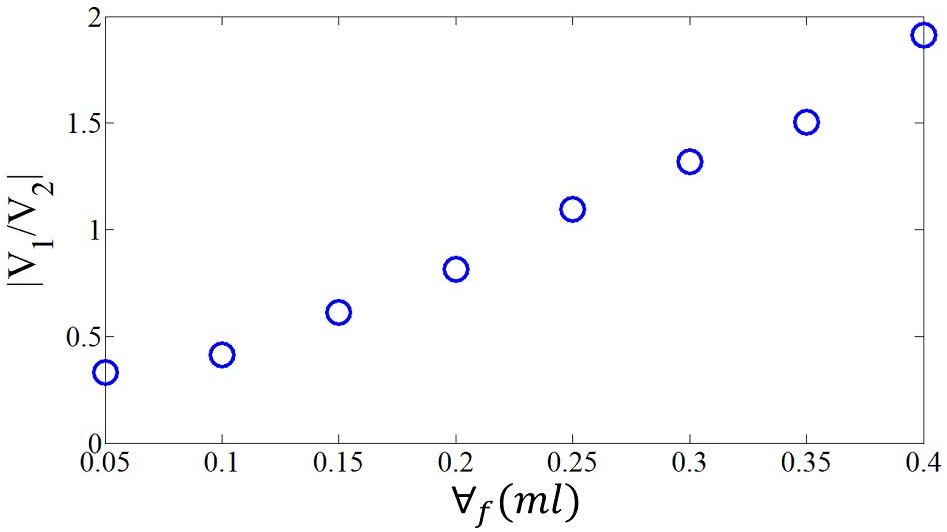

Figure 8: Ratio of positive and negative peak EMF values ($|V_1/V_2|$) for various volumes of ferrofluid drop ($\forall_f$) driven by 6 magnets ($N = 6$).